Pressure-induced structural phase transition in LiV_2O_4

L. Pinsard-Gaudart,[1] N. Dragoe,[1] P. Lagarde,[2] A. M. Flank,[2] J. P. Itie,[2] A. Congeduti,[2] P. Roy,[2] S. Niitaka,[3] and H. Takagi[3]
[1]*ICMMO, Université Paris Sud, UMR 8182-CNRS, 91405 Orsay, France*
[2]*Synchrotron SOLEIL, CNRS-UR1, l'Orme des merisiers, 91192 Gif-sur-Yvette, France*
[3]*RIKEN (The Institute for Physical and Chemical Research), Wako 351-1098, Japan*
(Received 8 February 2007; revised manuscript received 13 April 2007; published 30 July 2007)

Extended x-ray absorption fine structure analysis of LiV_2O_4 at the vanadium *K* edge under pressure is discussed. Changes in the absorption spectra at room temperature show that a structural phase transition is induced at high pressure. This phase transition can be attributed to a charge ordering, as it was observed in the isostructural compound AlV_2O_4. The absorption spectra have been analyzed by considering the two models previously proposed for AlV_2O_4. Our results indicate that the high pressure structure of LiV_2O_4 is probably implying the formation of "vanadium molecules" in a geometrically frustrated crystal.

DOI: 10.1103/PhysRevB.76.045119 PACS number(s): 87.64.Fb, 75.30.Mb, 74.62.Fj

I. INTRODUCTION

Among a wide variety of structural categories of transition metal oxides, the spinel, generally expressed by the chemical formula AB_2O_4, is unique in that an unusually strong geometrical frustration on both "spin" and "charge" channels is anticipated from its pyrochlore type-*B* sublattice.[1] When the *B* site is occupied by vanadium ions with orbital degeneracy, complex electronic and magnetic properties emerge.[2] For instance, with divalent ions at the tetrahedral *A* site, the *B* site has integral valence, giving rise to Mott insulating behavior with frustrated magnetism, e.g., in ZnV_2O_4.[2] On the other hand, LiV_2O_4, with monovalent *A* site ions and mixed-valence V 3.5+ ions, exhibits heavy fermion behavior at low temperatures with an unexpected large specific heat coefficient, which, surprisingly, is comparable to those of intermetallic heavy fermions such as UPt_3 and $CeCu_2Si_2$.[3] Several related compounds have been studied, for instance, AlV_2O_4,[4] having spinel structure and thus geometrically frustrated.

LiV_2O_4 has a face-centered-cubic, normal-spinel structure with the space group $Fd-3m$,[5] and the formal oxidation state of the V ion is 3.5+. Since LiV_2O_4 is a mixed-valence compound, it is highly likely that the heavy mass electrons crystallize into a charge ordered state. If this is the case, the heavy fermion state at ambient pressure can be viewed as a melted electron crystal. Previous studies showed that LiV_2O_4 remains cubic down to low temperature, indicating that all V sites are crystallographically equivalent and no magnetic ordering occurs above 20 mK.[3] A metal-insulator (MI) transition at low temperatures and under high pressures has been suggested for this compound, based on electrical properties data.[6] The electrical resistivity of LiV_2O_4 shows a metallic behavior below about 5 GPa, with an upturn indicating an insulator when raising the pressure and decreasing the temperature. The temperature of this transition depends on the pressure applied: it is about 125 K at 7 GPa and 150 K at 8.5 GPa (the highest applied pressure for these resistivity measurements). From these results, it could be anticipated that a MI transition would occur at RT if the applied pressure is high enough. The MI transition could be attributed to charge ordering of V ions, as observed in the isostructural AlV_2O_4. Two charge ordered structures proposed for the aluminum derivative, both as transitions from $Fd-3m$ to an $R-3m$ space group, are presented in Table I: (i) a charge ordering consisting of the formation of three $V^{2.5-x}$ ions and one $V^{2.5+3x}$ ion coupled with a rhombohedral distortion along the [111] axis (called hereafter a *three-one* type, model I)[7] [Fig. 1(a)] and (ii) complex distortion involving the formation of a cluster of seven vanadium atoms (a *heptamer*, model II), proposed recently by Horibe *et al.*[8] [Fig. 1(b)].

A charge ordered phase in LiV_2O_4, i.e., the electron crystallization state, could presumably be of the same type as one can observe in AlV_2O_4 which also has a spinel structure. The main difference between the two models, other than the doubling of the lattice parameter, is in the charge order.

From a structural viewpoint the three-one transition implies a contraction of the kagome plane, V1 atoms, so a decrease of the V1–V1 distances. For the heptamer structure, the distortion is more complex and implies both decreases and increases of the V-V distances. There are six V-V distances spread over more than 0.5 Å. Of particular importance for the discussion hereafter are the V3–V3 distances in the kagome plane of the heptamer model. A shift of V ion in this plane is manifesting as increase of some V3–V3 distances and decrease of other V3–V3 distances (3.14 and 2.61 Å for the AlV_2O_4 case, Table I). We will use these structural features in the data analysis (see later).

In a recent study, it has been inferred from powder x-ray diffraction under high pressure and low temperature (10 K) that LiV_2O_4 would present a similar behavior as model I of AlV_2O_4, which is a three-one-type distortion.[9]

In order to determine the local symmetry of vanadium in LiV_2O_4, extended x-ray absorption fine structure (EXAFS) analysis at the vanadium *K* edge was performed for pressures up to 21.7 GPa at room temperature.

II. EXPERIMENTAL METHOD

The samples were powdered single crystals grown by a flux method similar to that reported recently.[10] X-ray diffraction on the obtained single crystals confirmed the proposed structure, $Fd-3m$ space group, and gave a lattice parameter $a=8.227$ Å at $R=1.9\%$. This value was considered for the

 ©2007 The American Physical Society

TABLE I. Structural details of AlV_2O_4 and LiV_2O_4.

	AlV_2O_4			LiV_2O_4
Symmetry	$Fd-3m$[a]	$R-3m$ (I)[b]	$R-3m$ (II)[c]	$Fd-3m$
Cell	a=8.19 Å	a_R=5.8438, α=58.975°[d]	a_H=5.75 Å, c_H=28.85 Å	a=8.227 Å
V positions	8a	V1 in 3d, V2 in 1a	V1 in 3a, V2 in 3b, and V3 in 18h[e]	8a
V-O distances (Å)	V-O: 2.04 (×6)	V2-O: 2.01 (×6)	V1-O: 2.04 (×6)	V-O: 1.97 (×6)
			V2-O: 2.02 (×6)	
		V1-O: 2.05 (×4)	V3-O: 2.02 (×2)	
			V3-O: 2.04 (×1)	
		V1-O: 2.06 (×2)	V3-O: 2.10 (×3)	
V-V distances (Å)	V-V: 2.89 (×6)	V2-V1: 2.92 (×6)	V1-V3: 3.04 (×6)	V-V: 2.91 (×6)
		V1-V1: 2.87 (×4)	V2-V3: 2.81 (×6)	
		V1-V2: 2.92 (×2)	V3-V3: 2.61 (×2)	
			V2-V2: 2.80 (×1)	
			V1-V3: 3.03 (×1)	
			V3-V3: 3.14 (×2)	

[a]Reference 4.
[b]Reference 7.
[c]Reference 8.
[d]In hexagonal setting: a_H=5.753 Å and c_H=14.424 Å.
[e]Note the different multiplicities for the V atoms: there are six oxygen atoms located at 2.04 Å distance from V1, so there are 18 V1-O bonds and 18 V2-O bonds, and 54 short V3–O bonds and 54 long V3-O bonds. In terms of the coordination numbers (CNs) given in Table III, we can consider globally two V-O distances with CNs of 2.25 and 3.75 corresponding to 54 longer V3–O bonds and 90 shorter V-O bonds, respectively.

calculation of the distances (see Table I) and is in good agreement with a previous study.[5]

For EXAFS measurements, powder samples were loaded in preindented Inconel alloy gaskets of about 20 μm thickness in a membrane-type diamond anvil cell (DAC) with silicon oil as pressure transmitting medium. The pressure was measured by using the ruby fluorescence method. The measurements were performed at the K edge of vanadium (5465 eV) in transmission mode from 5400 to about 5900 eV, at room temperature, and up to 21.7 GPa. Because of the absorption of diamond, classical anvils are not adapted at this energy. In order to reduce the strong absorption of diamond, perforated anvils have been adapted in the DAC in order to reduce the path length in diamond (0.5 mm thick miniature anvils with 0.2 mm culet diameter have been glued to perforated anvils).[11] The experiments were performed at Paul Scherrer Institute at the SLS LUCIA beamline using a Si (111) monochromator.[12] At least two scans were performed for each pressure. Data treatment was performed using the IFEFFIT[13] and FEFF8 packages.[14]

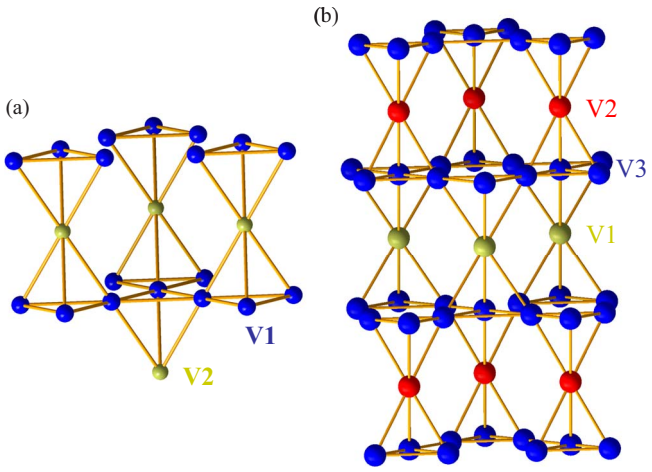

FIG. 1. (Color online) Charge ordering structures of AlV_2O4: (a) three-one type and (b) heptamer type.

III. RESULTS AND DISCUSSION

Raw EXAFS spectra of LiV_2O_4 under several pressures are shown in Fig. 2. The useful data are limited to 5900 eV by monochromator glitches which are not fully compensated. The overall decrease of the absorption of the sample with pressure corresponds to a gradual packing of the powder. As it can be seen from the absorption spectra obtained at pressures ranging from 0.7 to 21.7 GPa, there is a definite evolution of the absorption oscillations within the pressure domain around 10 GPa. Other changes induced by pressure are observed near the edge region, but we postpone their discussion to the second part of the analysis.

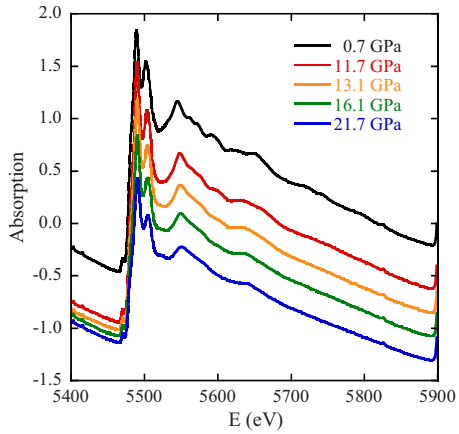

FIG. 2. (Color online) Selected absorption spectra of LiV_2O_4 at the vanadium K edge as a function of pressure.

A. Extended x-ray absorption fine structure analysis

The data analysis has been done in a conventional way, that is to say, a modeling of the atomic background with a degree 5 polynomial, between 5486 and 5874 eV, and a normalization using the Heitler formula. The Fourier transforms are k^3 weighted (Fig. 3). The apodization window is of the Hanning type between 1.7 and 9.5 $Å^{-1}$. A back Fourier filtering has then been applied within the 0.9–3.5 Å R window. The first peak observed in the radial distribution function, at about 1.4 Å, corresponds to the oxygen environment of the vanadium. Larger distances, around 2.3 Å (uncorrected from phase shifts), are dominated by the V-V bonds and probably other contributions from V-Li and from multiple scattering paths.

By increasing the pressure, up to about 12 GPa, one can notice (i) an increase (by about 30%) of the amplitude of the first peak and (ii) a gradual decrease of the intensity and a shift of the peak position corresponding to the second coordination sphere (about 2.3 Å in Fig. 3). This change can be attributed to a phase transition, as it was proposed based on low temperature resistivity and x-ray diffraction measurements. We note that this transition takes place at room temperature.

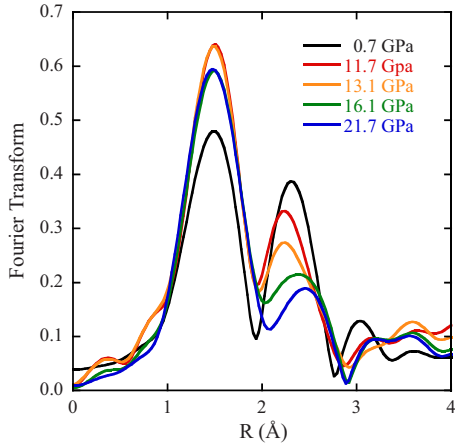

FIG. 3. (Color online) Radial distribution functions at different pressures.

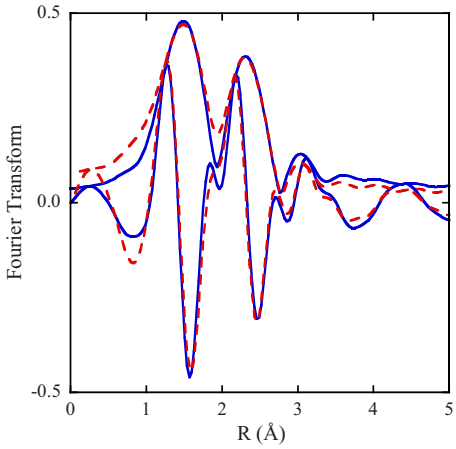

FIG. 4. (Color online) Fit of the Fourier transform of the 0.7 GPa data (amplitude and imaginary parts). Solid line: experiment, dotted line: fit.

In order to understand the changes observed under pressure, quantitative analysis has been performed. A fitting procedure has then been undertaken where the coordination numbers and interatomic distances are fixed parameters, and the only free parameters are the disorder terms since they are not taken into account by the FEFF calculation. The fit has been applied to a filtered signal of the Fourier transform between R=0.5 Å and R=3 Å, the k space spanning from 2.5 to 9 $Å^{-1}$. Within these mathematical conditions, the number of free parameters allowed in the fitting procedure amounts to around 12; we have included the first eight paths up to R_{eff}=3.62 Å (including double scattering paths where vanadium intervenes between the central vanadium atom and an oxygen atom). For the analysis of the low pressure phase, assumed to be the cubic one ($Fd-3m$), the edge energy shift was refined, and the value obtained by this fit has then been fixed during the analysis of the other structures since the experimental data do not evidence any significant edge shift in terms of EXAFS analysis. The inelastic parameter S_0^2 has been fixed to 0.8.

The results of the analysis for the low pressure phase are shown in Fig. 4 while Table II gathers the numerical values. In the first attempt, we checked if the cubic structure could be a possible solution for the high pressure results. The fit-

TABLE II. Structural results obtained for the low pressure phase. The edge energy is 5478.4 eV.

R (fixed) (Å)	CN (fixed)	$\sigma^2 \pm 0.0005$ ($Å^2$)
1.97 (V-O)	6	0.004
2.91 (V-V)	6	0.005
3.29 (V-O-O)	12	0.088
3.40 (V-O)	2	0.044
3.41 (V-Li)	6	0.001
3.42 (V-V-O)	24	0.033
3.43 (V-O-O)	12	0.001
3.62 (V-O)	6	0.021

TABLE III. Structural results obtained for the high (21.7 GPa) pressure phase by considering model II. The coordination numbers were fixed at values obtained from structural model II by taking into account the different vanadium sites and their multiplicities.

$R\pm0.01$ (Å)	CN (fixed)	$\sigma^2\pm0.0005$ (Å^2)
1.91 (V-O)	3.75	0.001
2.00 (V3–O)	2.25	0.001
2.66 (V3–V3)	1.5	0.051
2.73 (V-V)	1.5	0.026
2.96 (V-V)	1.5	0.001
3.08 (V3–V3)	1.5	0.040

ting procedure definitely rejects this hypothesis. Then, the analysis of the high pressure phase has been done assuming two possible structures, the three-one $R-3m$ (I) one and the heptamer $R-3m$ (II) (see Table I) and replacing aluminum atoms by lithium. The coordination numbers (N) were fixed according to each model.

Since there is no charge ordered phase known for LiV_2O_4, we used the same models as those proposed for AlV_2O_4 and listed in Table I, but small changes in the distances should be expected. We first consider the first model (I), taking into account the following structural constraints for the first five paths around vanadium and starting from the values listed in Table I for AlV_2O_4: (i) the same variation is imposed to the V1–O and V2–O interatomic distances and (ii) an opposite variation is imposed to the V1–V2 and V2–V1 distances. While the numerical result of the fit reaches good figures, in terms of residuals, it never delivers a full set of physical reasonable values (distances and Debye-Waller factors), in particular, the V2–V2 distances become 3.68 Å, which is incompatible with the structural transition considered.

For the second model, a similar analysis gave the results presented in Table III. As in the preceding case, from the heptamer model presented in Table I, several constraints have been applied to the fit. The changes of the V-O distances have to be identical, the variations of the V3–V3 distances located in the heptamer plane are of opposite signs because the structural distortion implies a shift of V3 ion in the kagome plane, and finally, the Debye-Waller factor of these two distances are kept identical. A shift of V3 ion in this plane (see Fig. 1) is manifesting as an increase of one V3–V3 distance and a decrease of the other V3–V3 distance: from 3.14 and 2.61 Å for the AlV_2O_4 case, we obtain here 3.09 and 2.66 Å, respectively. The quality of the fit, shown in Fig. 5, can be seen by the agreement between the experimental and theoretical Fourier transforms.

The EXAFS analysis, particularly the behavior of the second coordination shell of the vanadium atoms, definitely supports the hypothesis of a pressure transition of LiV_2O_4 to an $R-3$(II) structure above about 12 GPa.

Keeping the energy edge shift and the S_0^2 parameter constant in the analysis are very crude approximations in the case of the high pressure phase of LiV_2O_4, which is known to present a charge ordering behavior, with different valences for each of the three vanadium types of atoms. Actually,

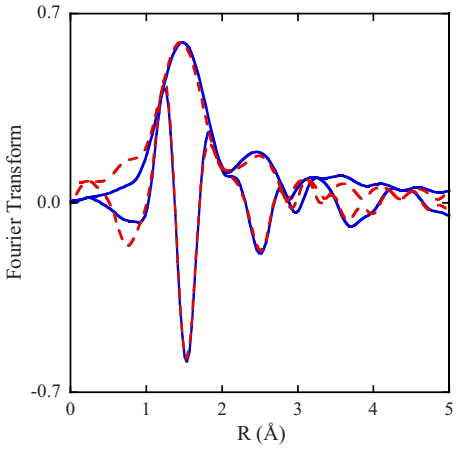

FIG. 5. (Color online) Fit of the Fourier transform of the 21.7 GPa data (amplitude and imaginary parts) using the structural values listed in Table III. Solid line: experiment, dotted line: fit.

allowing the edge energy to vary does not change much the results of the fit. Moreover, the overall structure of the lattice changes drastically through the transition. Therefore, the numerical results should not be considered as "true" structural values but only a proof that a change with pressure is going toward a heptamerlike structure.

B. First shell and near edge analysis

In order to detect more accurately the transition pressure, we performed a fitting procedure of the V-O distances by using the cubic phase model for the whole pressure range. FEFF gives all the scattering phase and amplitude files well known as "feff000x" files which describe the contributions of the elemental scattering paths contributing to the EXAFS signal. We then analyzed only the first peak in the Fourier transform (by considering only one distance and one Debye-Waller term) from a filtered signal of the Fourier transform between $R=1$ Å and $R=2$ Å. The energy shift and S_0^2 parameter were fixed to the values obtained at low pressure. Figure 6 shows the evolution with the pressure for the distance and the disorder term. Note that at higher pressure, these parameters have no direct meaning since the fit was done by considering only a single oxygen shell. However, other than a global V-O interatomic distance decrease with pressure, we can observe that (i) there is a gradual decrease of the V-O distances up to about 6 GPa, (ii) the V-O distance remains almost constant but, more important, a strong variation of the Debye-Waller term occurs between 6 and 11 GPa, and (iii) there is another slow decrease in the VO distances above about 12 GPa.

Between 6 and 12 GPa, a definite change of the crystallographic structure is evidenced by the behavior of both the V-O interatomic distance and the Debye-Waller factor: the V-O distance stays almost constant while the disorder parameter undergoes a strong increase. The Fourier transforms of a limited set of pressures around this domain are shown in Fig. 7(b), where this behavior appears clearly on the relative amplitudes of the peaks. It seems that the entire structure is strongly modified between 6 and 9.8 GPa, followed by a

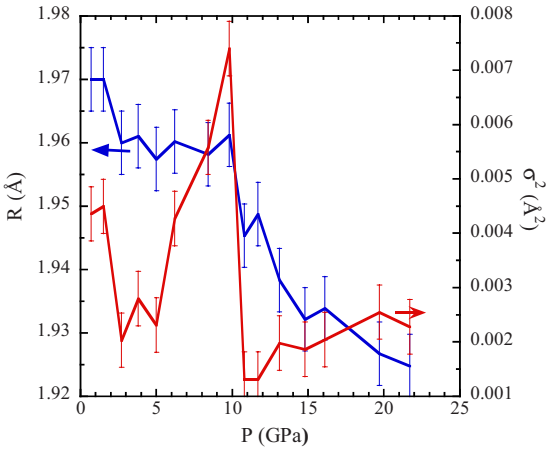

FIG. 6. (Color online) Calculation of the first V-O distances and disorder terms for LiV_2O_4 at various pressures, calculated within a single shell model.

rearrangement of the oxygen environment between 9.8 and 11.7 GPa (the amplitude of the first peak sharply increases to reach the value it will keep until 21.7 GPa and the disorder parameter drops). Then, at higher pressures, modification of the middle range order toward its final structure occurs. The phase transition then appears very complicated. In comparison with the data obtained by electrical resistivity, this value

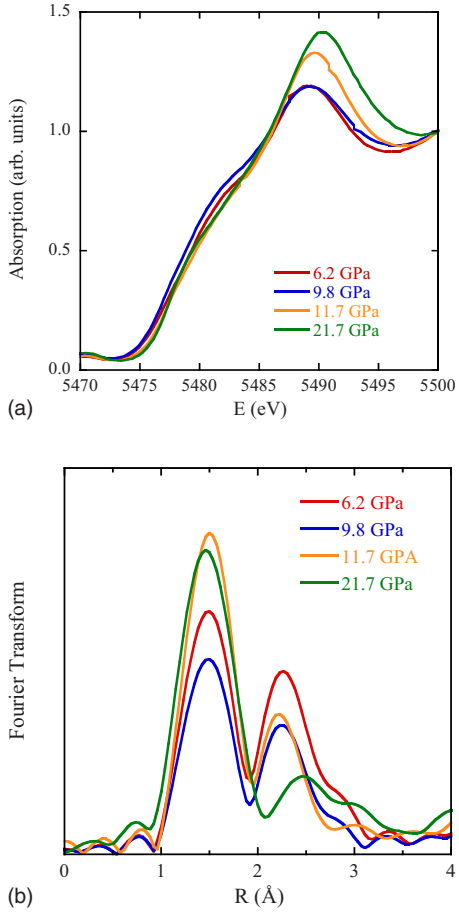

FIG. 7. (Color online) (a) Absorption spectra and (b) Fourier transforms at various pressures.

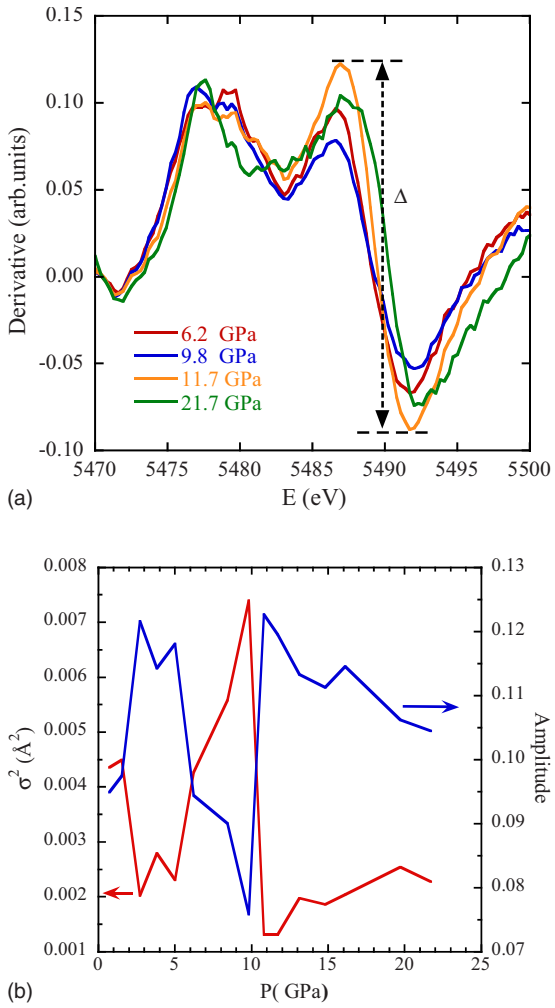

FIG. 8. (Color online) (a) Derivative of the absorption spectra. (b) Disorder term for the first shell and amplitude of the absorption spectra derivative as a function of the applied pressure.

of the pressure at which the structural phase transition would take place is rather low. This can be explained by the difference in the detection scale for the EXAFS and resistivity techniques. EXAFS measurements are more sensitive to this kind of transition because there is no need for an extensive domain to observe a structural change. On the contrary, electrical resistivity measurements are biased by the existence of a percolation level, and therefore more sensitive to the long-range order. We can conclude from these data that a phase transition starts at about 6 GPa and it is completed at about 12 GPa.

The XANES part presents also changes that we now analyze in comparison with the above EXAFS results. The derivatives of the spectra between 5470 and 5500 eV for some selected pressures are shown in Fig. 8(a). The evolution is small between 0.7 and 6.2 GPa; then, a strong modification takes place between 6.2 and 10.8 GPa while the evolution above 11.7 until 21.7 GPa will be smooth again. The white line is located at about 5489 eV and Fig. 8(b) compares the behavior with pressure of the first shell Debye-Waller factor (already shown in Fig. 6) and the amplitude of the derivative [△ in Fig. 8(a)] of the white line, a quantity directly related

to the intensity of this white line. The *K*-edge white line intensity is directly related to the energy width of the first available *p*-state band, which is, in turn, related to the distortion of the first coordination shell. This is especially true in oxide compounds where the oxygen first shell in a quasioctahedral configuration around the V atom builds a quasimolecular state. The striking correlation between the two curves which are issued from two independent data analysis reinforces the description of the phase transition obtained from the first shell analysis only.

While the phase transition of LiV_2O_4 under pressure should be similar to the one observed at 700 K for the AlV_2O_4, the interatomic distances are rather different for the two compounds. This is in line with the formal valence state for vanadium in the two compounds, which is 2.5+ for aluminum and 3.5+ for lithium derivative. We can expect that the interatomic distances and V-O, in particular, are smaller for the lithium derivative than for the aluminum one since the crystal radii for vanadium in octahedral configuration are 0.93, 0.78, and 0.72 Å for V^{2+}, V^{3+}, and V^{4+}, respectively.[15] This suggests that the V-O distances should be about 0.1 Å different for the two structures, which is indeed the case (see Table I and the EXAFS results). For the case of charge ordering phases for the two compounds, based on the same type of argument, it would imply a stronger splitting of the distances for the $V^{2.5+}$ than for the $V^{3.5+}$. Indeed, EXAFS results show that the splitting of the V3–V3 distance is smaller for the LiV_2O_4 than for AlV_2O_4 (3.08 and 2.66 Å compared to 3.14 and 2.61 Å, respectively).

Finally, it is worth to point out from Fig. 6 that the Debye-Waller term appears lower at high pressure than at 0.7 GPa despite the large spread of V-O distances in the heptamer model (see Table I). This can be understood remembering that the photoabsorption is a very fast process which takes a "snapshot" of the crystal structure. In the low pressure metallic phase, all vanadium atoms are crystallographically equivalent with a formal valence of 3.5^+. In terms of EXAFS, this corresponds to equal populations of V^{3+}–O and V^{4+}–O split by about 0.07 Å, plus a thermal disorder (typically 0.05 Å) which is superimposed to this "structural" one. In the high pressure phase, these V-O distances are splitted into two groups, one around 1.91 Å, with an apparent coordination number of 3.75, and another one at 2 Å concerning 2.25 V3 atoms. The corresponding distribution is, therefore, narrower and this translates into a smaller Debye-Waller factor although the low pressure phase could appear more symmetric.

IV. CONCLUSIONS

EXAFS experiments under pressure above 12 GPa revealed a phase transition at room temperature probably related to a charge ordered state. Based on our results, the LiV_2O_4 structure should not be very different from that of the heptamer model of AlV_2O_4, with the exception of the changes induced by the vanadium oxidation state. Contrary to the aluminum phase, in the LiV_2O_4, the vanadium has an average valence of $3.5+(3d^{1.5})$ and this induces changes in the V-O and V-V distances, as well as the electron distribution in this "molecule." At a first glance, similarities between these compounds suggest that the driving force for this transition is the geometrically frustrated state. Further work is necessary, particularly x-ray diffraction under pressure, to determine precisely the structural parameters and to understand the charge ordered state in the LiV_2O_4 compound.

ACKNOWLEDGMENTS

This research project has been supported by the European Commission under the sixth Framework Programme through the Key Action "Strengthening the European Research Area: Research Infrastructures," Contract No. RII3-CT-2004-506008. This work was performed at the Swiss Light Source, Paul Scherrer Institute, Villigen, Switzerland. We are grateful to the machine and beamline groups whose outstanding efforts have made these experiments possible.

[1] P. W. Anderson, Phys. Rev. **102**, 1008 (1956).
[2] M. Onoda, H. Imai, Y. Amako, and H. Nagasawa, Phys. Rev. B **56**, 3760 (1997).
[3] S. Kondo *et al.*, Phys. Rev. Lett. **78**, 3729 (1997); C. Urano, M. Nohara, S. Kondo, F. Sakai, H. Takagi, T. Shiraki, and T. Okubo, *ibid.* **85**, 1052 (2000).
[4] B. Reuter, R. Aust, G. Colsmann, and C. Neuwald, Z. Anorg. Allg. Chem. **500**, 188 (1983).
[5] B. Reuter and J. Jaskowski, Angew. Chem. **72**, 209 (1960); Y. Matsushita, J. Yamaura, and Y. Ueda, J. Des. Manuf. **E61**, i137 (2005).
[6] C. Urano, Ph.D. thesis, University of Tokyo, 2003.
[7] K. Matsuno, T. Katsufuji, S. Mori, Y. Moritomo, A. Machida, E. Nishibori, M. Takata, M. Sakata, and H. Takagi, J. Phys. Soc. Jpn. **70**, 1456 (2001); K. Matsuno *et al.*, Phys. Rev. Lett. **90**, 096404 (2003).
[8] Y. Horibe *et al.*, Phys. Rev. Lett. **96**, 086406 (2006).
[9] K. Takeda *et al.*, Physica B **359-361**, 1312 (2005).
[10] Y. Matsushita, H. Ueda, and Y. Ueda, Nat. Mater. **4**, 845 (2005).
[11] A. Dadashev, M. P. Pasternak, G. K. Rozenberg, and R. D. Taylor, Rev. Sci. Instrum. **72**, 2633 (2001); J. P. Itié, F. Baudelet, A. Congeduti, B. Couzinet, F. Farges, and A. Polian, J. Phys.: Condens. Matter **17**, S883 (2005).
[12] A.-M. Flank *et al.*, Nucl. Instrum. Methods Phys. Res. B **246**, 269 (2006).
[13] M. Newville, J. Synchrotron Radiat. **8**, 322 (2002).
[14] A. L. Ankudinov, B. Ravel, J. J. Rehr, and S. D. Conradson, Phys. Rev. B **58**, 7565 (1998).
[15] R. D. Shannon, Acta Crystallogr., Sect. A: Cryst. Phys., Diffr., Theor. Gen. Crystallogr. **A32**, 751 (1976).